$\mathcal{M}_{i\mathbb{N}}\mathcal{E}$

Research article

Multiphase modelling of glioma pseudopalisading under acidosis[†]

Pawan Kumar[1], Christina Surulescu[1,*] and Anna Zhigun[2]

[1] Felix-Klein-Zentrum für Mathematik, Technische Universität Kaiserslautern, Paul-Ehrlich-Str. 31, 67663 Kaiserslautern, Germany

[2] School of Mathematics and Physics, Queen's University Belfast, University Road, Belfast BT7 1NN, Northern Ireland, UK

[†] **This contribution is part of the Special Issue:** Advances in the analysis of chemotaxis systems
Guest Editor: Michael Winkler
Link: www.aimspress.com/mine/article/6067/special-articles

* **Correspondence:** Email: surulescu@mathematik.uni-kl.de.

Abstract: We propose a multiphase modeling approach to describe glioma pseudopalisade patterning under the influence of acidosis. The phases considered at the model onset are glioma, normal tissue, necrotic matter, and interstitial fluid in a void-free volume with acidity represented by proton concentration. We start from mass and momentum balance to characterize the respective volume fractions and deduce reaction-cross diffusion equations for the space-time evolution of glioma, normal tissue, and necrosis. These are supplemented with a reaction-diffusion equation for the acidity dynamics and lead to formation of patterns which are typical for high grade gliomas. Unlike previous works, our deduction also works in higher dimensions and involves less restrictions. We also investigate the existence of weak solutions to the obtained system of equations and perform numerical simulations to illustrate the solution behavior and the pattern occurrence.

1. Introduction

Glioblastoma is the most common type of primary brain tumors in adults, with a dismal prognosis. The histological features include characteristic patterns called pseudopalisades, which exhibit garland-like structures made of aggregates of glioma cells stacked in rows at the periphery of regions with low pH and high necrosis surrounding the occlusion site(s) of one or several capillaries [39]. Such patterns

are used to grade the tumor and are essential for diagnosis [6, 23].

The few continuous mathematical models proposed for the description of pseudopalisade patterns [1, 26, 27, 30], involve systems of ODEs and PDEs which were set up in a heuristic manner or obtained from lower scale dynamics. They account for various aspects like phenotypic switch between proliferating and migrating glioma as a consequence of vasoocclusion and nutrient suppression associated therewith [1], interplay between normoxic/hypoxic glioma, necrotic matter, and oxygen supply [30], or tissue anisotropy and repellent pH-taxis, with [27] or without [26] vascularisation. The latter two works deduced effective equations for glioma dynamics from models set on the lower, microscopic and mesoscopic scales in the kinetic theory of active particles (KTAP) framework explained e.g., in [4]. Those deductions are in line with previous works concerning glioma invasion in anisotropic tissue [9–11, 14–16, 18, 31], which use parabolic scaling to obtain the equations for glioma evolution on the macroscale from descriptions of subcellular and mesoscopic dynamics. Here we propose yet another approach, relying on the interpretation of the relevant components (glioma, normal tissue, necrotic matter, and acidity) as phases in a mixture - with the exception of acidity, which is characterised by proton concentration in the volume occupied by the phases.

Multiphase models in the framework of mixture theory [2, 12] have been considered in connection with cancer growth and invasion, (arguably) starting with [7, 8] and followed by many others, involving different mathematical and biological aspects; see e.g., [17, 19, 32–34, 36, 37, 40] and references therein. Particularly [34] provides a comprehensive discussion of the classes of multiphase models, along with their strengths and drawbacks. Such models employ a population level description with conservation laws analogous to balance equations for single cells, with supplementary terms accounting for interphase effects. Thereby, the living cells and tissues are most often seen as viscous fluids, while the interstitial fluid is inviscid. Few of the existing models (e.g., [17, 34, 40]) are explicitly handling necrosis, which is, however, an important component of advanced tumors. Likewise, there are relatively few models accounting for chemoattracting or chemorepellent agents (e.g., [17, 37]), which are known to bias in a decisive way the expansion of the neoplasm and therewith associated dynamics of tumor cells and surrounding tissue. To our knowledge there are no multiphase models for glioma pseudopalisade development. In this context we propose such a model comprising necrotic matter as one of the phases in the mixture (although there are a few issues related to this approach, as mentioned, e.g., in [34]). As our main aim is to describe glioma behavior in an acidic environment fastly leading to extensive necrosis, we explicitly include these influences in our model. From the mass and momentum balance equations written for the phases composing the neoplasm and supplemented with appropriate constitutive relations, we then deduce, under some simplifying assumptions, a system of reaction-cross diffusion equations with repellent pH-taxis for the glioma cells and normal and necrotic tissues, also including a solenoidality constraint on the total flux. Our deduction has some similarities with that in [19], however is done in N dimensions instead of 1D, it accounts explicitly for the evolution of necrotic matter and the effects of acidity, and does not require the drag coefficients between the phases to be equal. The obtained equations are able to reproduce qualitatively the typical pseudopalisade patterns with all their aspects related to the glioma aggregates, acidity, necrotic inner region, normal tissue dynamics.

The rest of this paper is organized as follows: Section 2 contains some notations and conventions. Section 3.1 contains the model setup with the considered phases (glioma cells, normal tissue, necrotic

matter, and interstitial fluid) and the corresponding mass and momentum balance equations, along with their associated constitutive relations. That description is used to deduce the announced reaction-cross diffusion equations. Thereby, we investigate a model with an immovable component and observe that enforcing one of the phases to be fixed prevents the simultaneous validity of all basic conservation laws needed in the setting. Then we neglect the interstitial fluid, thus reducing the number of phases, and obtain the PDEs with reaction, nonlinear diffusion and taxis terms, while still ensuring all balance equations. The total flux needs to be given, satisfying a solenoidality constraint. Section 4 is dedicated to the existence of weak solutions to the obtained cross diffusion system coupled with the reaction-diffusion equation for acidity dynamics in the volume of interest. Finally, in Section 5 we provide numerical simulations for that system, studying several parameter scenarios in order to put in evidence the effect of acidity and of different drag coefficients on the obtained patterns exhibiting pseudopalisade formation.

2. Preliminaries

We will use the following notation throughout this paper:

Notation 2.1. 1) By vector we always mean a column vector.

2) We denote by e the vector of length 4 and all components equal to one. As usual, I_l stands for the identity matrix of size l.

3) For two vectors $w^{(1)}$ and $w^{(2)}$ of the same length we denote by $w^{(1)}.w^{(2)}$ the vector with elements $w_i^{(1)} w_i^{(2)}$. Similarly, for a vector w with nonzero elements we write $w.^{-1}$ meaning the vector with coordinates w_i^{-1}.

4) For a vector w we denote by $\text{diag}(w)$ the diagonal matrix with $(\text{diag}(w))_{ii} = w_i$.

5) As usual, $\cdot$ denotes the scalar product.

6) As usual, ∇ refers to the gradient with respect to the spatial variable x.

Notation 2.2. Throughout the paper we often skip the arguments of coefficient functions.

3. Modelling

3.1. Model setup

Model variables Motivated by the multiphase approach developed in [19] we view the tumour and its environment as a saturated mixture of several components. We assume these components to be: tumour cells, normal tissue (mainly the extracellular matrix, but also normal cells), necrotic tissue (was not included in [19]), and interstitial fluid. The latter, in turn, has several constituents, among which are protons. Depending on their concentration, the environment can be more or less acidic. pH levels drop due to enhanced glycolytic activity of neoplastic cells. We assume that neither cells nor living tissue are produced due to an already very acidic, and hence very unfavourable, environment. Thus we assume that the total volume of the mixture is preserved, the phases only transferring from one into another. The main variables in our models, all depending on time $t \geqslant 0$ and position in space $x \in \Omega \subset \mathbb{R}^N$, Ω a domain, are:

- vector $u : [0, \infty) \times \Omega \to [0, 1]^4$ of volume fractions of
    - tumour cells, u_c,
    - normal tissue, u_m,
    - necrotic tissue, u_n,
    - interstitial fluid, u_w.
- acidity (concentration of protons), $h : [0, \infty) \times \Omega \to [0, \infty)$.

Unlike [19] we do not require the space dimension, $N \in \mathbb{N}$, to be one. The main goal of this section is to derive equations for the volume fractions based primarily on the conservation laws for mass and momentum as well as additional assumptions on some of the phases. To write down the physical laws, we introduce additional variables that are subsequently eliminated. These are:

- fluxes of the components, $J_i : [0, \infty) \times \Omega \to \mathbb{R}^N$, $i \in \{c, m, n, w\}$,
- common pressure, $p : [0, \infty) \times \Omega \to \mathbb{R}$.

Model parameters The equations we develop below involve the following set of parameters:

- matrix of drag coefficients associated with each pair of components, $K \in \mathbb{R}^{4 \times 4}$;
- additional, isotropic pressures by the components, $\tau_i : [0, 1]^4 \times \mathbb{R} \to \mathbb{R}$, $i \in \{c, m, n, w\}$;
- reaction terms, $f_i : [0, 1]^4 \times \mathbb{R} \to \mathbb{R}$, $i \in \{c, m, n, w, h\}$;
- diffusion coefficient of the protons, $D_h > 0$.

Assumptions on K. We assume throughout that

$$K_{ij} > 0 \quad \text{and} \quad K_{ij} = K_{ji} \quad \text{for} \quad i, j \in \{c, m, n, w\}, \ i \neq j.$$

Assumptions on f_i's. In order to ensure that the sum of all volume fractions in the mixture is always one, we require

$$\sum_{i \in \{c, m, n, w\}} f_i \equiv 0. \tag{3.1}$$

Since u_i's and u_h should be nonnegative, we require further that

$$f_i \geqslant 0 \qquad \text{for } u_i = 0, \ i \in \{c, m, n, w\},$$
$$f_h \geqslant 0 \qquad \text{for } h = 0.$$

Possible choices for the reaction terms are:

Example 3.1. $f_c(u_c, u_n, h) = -c_1 u_c u_n (h - h_{max})$, $f_m(u_m, h) = -\frac{c_2 u_m (h - h_{max})_+}{1 + u_m + h} - c_3 u_m$, $f_n = -f_c - f_m$, $f_w = 0$. This accounts for the fact that the amount of both tissue and viable cancer cells (the latter being in interaction with the necrotic matter embedded in the acidic environment) decreases when the proton concentration h exceeds a certain maximum threshold, leading to acidosis and hypoxia. The tissue infers degradation due to causes other than direct influence of acidity or tumor cells, and, on the other hand, it experiences a certain amount of self-regeneration, which is limited by the already available tissue and low pH. Thereby, $c_1, c_2, c_3 > 0$ are constant rates; they could, however, also include further dependencies. For the reaction term in the acidity equation we choose e.g., $f_h = -a_1 u_w h / (1 + u_w h / h_{max}) + a_2 u_c - a_3 h$, with $a_i \geqslant 0$ $(i = 1, 2, 3)$ constants. This choice ensures proton uptake by the interstitial fluid (with saturation), production by glioma cells, and decay with rate a_3.

Assumptions on τ_i's. We assume that the non-living components (necrotic matter and extracellular fluid) acquire a tendency to reach equilibrium, so that only living matter exerts additional pressure, thus

$$\tau_n \equiv \tau_w \equiv 0. \tag{3.2}$$

The mechanical properties of living matter (tumour cells and normal tissue) are different; among others, they are able to generate both intra- and interphase forces in response to changes in the local environment. The influences include variations in the volume fraction of the cell phase and the presence of chemical cues, of which we account for the local acidity (via proton concentration). The corresponding forces manifest themselves as an additional intraphase pressure. It is assumed that the pressure in the tumour and normal tissue phases increases with their respective densities; moreover, glioma cells exert supplementary (isotropic) pressure on the normal tissue. Taking these effects into account, we choose for the additional pressure terms

$$\tau_c(u_c, h) := \alpha_c u_c + g(h), \qquad g(h) := \frac{\chi h}{1 + \frac{h}{h_{max}}}, \tag{3.3}$$

$$\tau_m(u_c, u_m) := \alpha_m(1 + \theta u_c)u_m, \tag{3.4}$$

where $\alpha_c, \alpha_m, \theta, h_{max}, \chi > 0$ are constants. In (3.3) we combine the influence of local cell mass and acidity, both adding to cancer cell pressure which, in turn, enhances glioma motility. Cell stress increases with growing cell mass, pushing the cells away from overcrowded regions. Stress due to acidity saturates for large acidity levels. Indeed, in highly acidic regions cell ion channels and pH-sensing receptors are mostly occupied, thus making cells insensitive to the presence of protons in their environment. As in [11, 24, 26, 27], we call this a repellent pH-tactic behaviour. Similarly, the choice in (3.4) means that there is some intraspecific tissue stress (compression) further accentuated by the interaction between glioma cells and their fibrous environment. The forms proposed in (3.3), (3.4) are reminiscent of those chosen in [19].

Main equations To derive our models we will rely on a set of equations describing physical laws. They are as follows.

- Since the the components of u are volume fractions, we have

$$\sum_{i \in \{c,m,n,w\}} u_i = 1. \tag{3.5}$$

  This is the so-called 'no void' condition.

- Mass conservation for ith component is given by

$$\partial_t u_i = -\nabla \cdot J_i + f_i. \tag{3.6}$$

  It would be reasonable to assume that this equation should hold for all phases. However, this may come into conflict with additional assumptions, see subsequent *Subsection 3.2*.

- Conservation of momentum for ith component is given by

$$-\nabla \cdot (u_i \sigma_i) = F_i, \tag{3.7}$$

where

$$\sigma_i = -(p + \tau_i)I_N \tag{3.8}$$

is the stress tensor involving the common pressure p and the additional pressure τ_i. It is assumed that the response of the tumour to stress is elastic and isotropic, which implies that the deformation induced by the applied force on each of the considered cellular and tissue components is limited. An unlimited deformation would correspond to a viscoelastic material [20], which is not considered here. The forms of the stress tensors depend on the material properties of each phase and their response to mechanical and chemical cues in the environment. As in [19, 28] the interstitial fluid is considered to be inert and isotropic and viscous effects within each phase are neglected.

The right hand side in (3.7) represents the force acting on the ith phase and, neglecting any inertial effects and exterior body forces, it takes the following form:

$$F_i = p\nabla u_i + \sum_{j \in \{c,m,n,w\}\setminus\{i\}} K_{ij}(u_i J_j - u_j J_i). \tag{3.9}$$

The first term on the right hand side in (3.9) accounts as usual (see, e.g., [7,19,28]) for the pressure distribution at the interface between phases. The remaining term represents viscous drag between the phases, with drag coefficients K_{ij}.

Plugging (3.8) and (3.9) into (3.7) yields an equation for the variables we introduced above:

$$\nabla \cdot (u_i(p + \tau_i)I_N) = p\nabla u_i + \sum_{j \in \{c,m,n,w\}\setminus\{i\}} K_{ij}(u_i J_j - u_j J_i). \tag{3.10}$$

Equation (3.10) is assumed to hold for all four phases.
- The proton concentration satisfies the reaction-diffusion equation

$$\partial_t h = D_h \Delta h + f_h. \tag{3.11}$$

In the remainder of this section we derive two models based on these laws. To begin with, we simplify Eq (3.10). Given that p and τ_i are scalar functions, we have for all $i \in \{c,m,n,w\}$

$$\sum_{j \in \{c,m,n,w\}\setminus\{i\}} K_{ij}(u_i J_j - u_j J_i) = \nabla \cdot (u_i(p + \tau_i)I_N) - p\nabla u_i$$

$$= \nabla(u_i(p + \tau_i)) - p\nabla u_i$$

$$= \nabla(u_i \tau_i) + u_i \nabla p. \tag{3.12}$$

Since K is symmetric, adding together the left-hand sides of (3.12) for all $i \in \{c,m,n,w\}$, we find that

$$\sum_{i \in \{c,m,n,w\}} \sum_{j \in \{c,m,n,w\}\setminus\{i\}} K_{ij}(u_i J_j - u_j J_i) = 0. \tag{3.13}$$

Combining (3.12) with (3.5) and (3.13), we obtain

$$0 = \sum_{i \in \{c,m,n,w\}} \nabla(u_i \tau_i) - u_i \nabla p$$
$$= \nabla(u \cdot \tau) + \nabla p,$$

so that

$$\nabla p = -\nabla(u \cdot \tau). \tag{3.14}$$

Plugging (3.14) into (3.12) we arrive at a system which no longer involves p:

$$\sum_{j \in \{c,m,n,w\} \setminus \{i\}} K_{ij}(u_i J_j - u_j J_i) = -u_i \nabla(u \cdot \tau) + \nabla(u_i \tau_i), \qquad i \in \{c,m,n,w\}, \tag{3.15}$$

and it holds that

$$\sum_{i \in \{c,m,n,w\}} (-u_i \nabla(u \cdot \tau) + \nabla(u_i \tau_i)) = 0. \tag{3.16}$$

Next, we introduce a matrix function

$$A : [0,1]^4 \to \mathbb{R}^{4 \times 4}, \qquad A_{im} := \begin{cases} -\sum_{j \in \{c,m,n,w\} \setminus \{i\}} K_{ij} u_j, & i = m, \\ K_{im} u_i, & i \neq m, \end{cases} \qquad i, m \in \{c,m,n,w\}. \tag{3.17}$$

The symmetry of K once again implies that

$$\sum_{i \in \{c,m,n,w\}} A_{im} \equiv 0, \qquad m \in \{c,m,n,w\}. \tag{3.18}$$

System (3.15) can now be written in the form

$$A J^{(l)} = -u \partial_{x_l}(u \cdot \tau) + \partial_{x_l}(\tau.u), \qquad l \in \{1, \dots, N\}, \tag{3.19}$$

where we denote by $J^{(l)}$ the vector made up of the lth coordinates of each J_i. Due to (3.16) and (3.18) for each l (at least) one equation is redundant. We exploit this in more detail in the next Subsections.

3.2. A model with an immovable component

Recall that u_m and u_n correspond to normal and necrotic tissues, respectively. A standard modelling assumption is that any tissue is completely immovable. This means that its flux is a zero function, turning the mass conservation law (3.6) into an ODE. However, as we show in this Section, already presupposing, e.g.,

$$J_n \equiv 0 \tag{3.20}$$

is problematic.

Singling out the nth phase, we use the following convenient notation.

Notation 3.2. For a vector y with components corresponding to the four phases we denote by $\tilde{y}$ the vector which is obtained by removing the component which corresponds to nth phase. Similarly, for a matrix A we denote by $\tilde{A}$ the submatrix which results from removing the row and column of A corresponding to that phase.

Recall that fluxes J_i, $i \in \{c, m, n, w\}$, satisfy system (3.19) which is underdetermined. We notice that the submatrix $\tilde{A}$ is diagonal-dominant due to (3.18) and the nonnegativity of u_i's and K_{ij}'s. Using the Gershgorin circle theorem, we infer that the real parts of the eigenvalues of $\tilde{A}$ do not exceed $-\rho_A(u_i)$, where

$$\rho_A := u_n \min_{i \in \{c,m,w\}} K_{ni}. \tag{3.21}$$

Therefore, for $u_n > 0$ the submatrix $\tilde{A}$ of A is invertible. Consequently, system (3.19)–(3.20) is uniquely solvable.

To simplify the calculations, let us now assume that the following technical assumption holds:

$$K = kk^T \quad \text{for some} \quad k \in [0, 1]^4. \tag{3.22}$$

In other words, the symmetric matrix K has rank one. One readily verifies the following formulas:

Lemma 3.3. *Let assumption* (3.22) *hold. Then:*

$$\tilde{A} = -(k \cdot u)\left(I_3 - \frac{1}{k \cdot u}(\tilde{k}.\tilde{u})\tilde{e}^T\right)\operatorname{diag}(\tilde{k}) \tag{3.23}$$

and

$$\tilde{A}^{-1} = -\frac{1}{k \cdot u}\operatorname{diag}^{-1}(\tilde{k})\left(I_3 + \frac{1}{k_n u_n}(\tilde{k}.\tilde{u})\tilde{e}^T\right), \tag{3.24}$$

so that

$$\tilde{A}^{-1}\tilde{w} = -\frac{1}{k \cdot u}\left(\tilde{k}.^{-1}.\tilde{w} + \frac{1}{k_n u_n}\tilde{u}(\tilde{e} \cdot \tilde{w})\right). \tag{3.25}$$

Using (3.25) we can resolve system (3.19)–(3.20) with respect to the components of the fluxes. For $l \in \{1, \dots, N\}$ and $i \in \{c, m, w\}$ we obtain

$$
\begin{aligned}
J_i^{(l)} &= -\frac{1}{k \cdot u}\left(\frac{1}{k_i}(-u_i\partial_{x_l}(u \cdot \tau) + \partial_{x_l}(u_i\tau_i)) + \frac{1}{k_n u_n}u_i\tilde{e} \cdot (-\tilde{u}\partial_{x_l}(u \cdot \tau) + \partial_{x_l}(\tilde{\tau}.\tilde{u}))\right) \\
&= -\frac{1}{k \cdot u}\left(\frac{1}{k_i}(-u_i\partial_{x_l}(u \cdot \tau) + \partial_{x_l}(u_i\tau_i)) + \frac{1}{k_n u_n}u_i(-(\tilde{e} \cdot \tilde{u})\partial_{x_l}(u \cdot \tau) + \partial_{x_l}(\tilde{u} \cdot \tilde{\tau}))\right) \\
&= -\frac{1}{k \cdot u}\left(\frac{1}{k_i}(-u_i\partial_{x_l}(u \cdot \tau) + \partial_{x_l}(u_i\tau_i)) + \frac{1}{k_n u_n}u_i(-(1 - u_n)\partial_{x_l}(u \cdot \tau) + \partial_{x_l}(\tilde{u} \cdot \tilde{\tau}))\right) \\
&= -\frac{1}{k \cdot u}\left(\frac{1}{k_i}(-u_i\partial_{x_l}(\tilde{u} \cdot \tilde{\tau}) + \partial_{x_l}(u_i\tau_i)) + \frac{1}{k_n}u_i\partial_{x_l}(\tilde{u} \cdot \tilde{\tau})\right) \\
&= -\frac{1}{k \cdot u}\left(\frac{1}{k_i}\partial_{x_l}(u_i\tau_i) - \left(\frac{1}{k_i} - \frac{1}{k_n}\right)u_i\partial_{x_l}(\tilde{u} \cdot \tilde{\tau})\right). \tag{3.26}
\end{aligned}
$$

We used (3.5) and (3.2) in the third and fourth equalities, respectively. Plugging (3.26) into (3.6) and using (3.2), we obtain

$$\partial_t u_i = \nabla \cdot \left(\frac{1}{k \cdot u} \left(\frac{1}{k_i} \nabla(u_i \tau_i) - \left(\frac{1}{k_i} - \frac{1}{k_n} \right) u_i \nabla(u_c \tau_c + u_m \tau_m) \right) \right) + f_i, \qquad i \in \{c, m\}, \qquad (3.27a)$$

$$\partial_t u_w = \nabla \cdot \left(\frac{1}{k \cdot u} \left(- \left(\frac{1}{k_w} - \frac{1}{k_n} \right) u_w \nabla(u_c \tau_c + u_m \tau_m) \right) \right) + f_w. \qquad (3.27b)$$

For variable u_n we have due to (3.6) and (3.20) that it satisfies an ODE:

$$\partial_t u_n = f_n. \qquad (3.28)$$

However, the structure of the fluxes in (3.27) would ensure (3.5) only if

$$\nabla \cdot \sum_{i \in \{c,m,w\}} J_i \equiv 0.$$

This condition fails to hold in general, unless for τ_c and τ_m such that

$$\sum_{i \in \{c,m,w\}} \left(\frac{1}{k_i} \nabla_u(u_i \tau_i) - \left(\frac{1}{k_i} - \frac{1}{k_n} \right) u_i \nabla_u(u_c \tau_c + u_m \tau_m) \right) = 0 \text{ for all } 0 \leqslant u_c, u_m, u_n, \sum_{i \in \{c,m,w\}} u_i \leqslant 1.$$
$$(3.29)$$

It is not fulfilled by the coefficients we have in mind, see *Subsection 3.1*.

Let us assume that (3.27) holds only for $i \in \{c, w\}$. Assume further that

$$u_w \equiv 0, \qquad (3.30)$$

i.e., that the liquid phase is negligible. In this case we obtain a haptotaxis model:

$$\partial_t u_c = \nabla \cdot \left(\frac{1}{k \cdot u} \left(\frac{1}{k_c} \nabla(u_c \tau_c(u, h)) - \left(\frac{1}{k_c} - \frac{1}{k_n} \right) u_c \nabla(u_c \tau_c(u, h) + (1 - (u_c + u_n)) \tau_m(u, h)) \right) \right)$$
$$+ f_c(u, h), \qquad (3.31a)$$
$$\partial_t u_n = f_n(u, h), \qquad (3.31b)$$
$$u_m = 1 - (u_c + u_n), \qquad (3.31c)$$
$$u = (u_c, u_m, u_n). \qquad (3.31d)$$

Unless τ_c is zero for $u_c + u_n = 1$, this model cannot ensure $u_m \geqslant 0$.

Altogether we see that trying to explicitly enforce an immovable phase leads to a situation where not all basic conservation laws can hold at the same time.

3.3. A model with total flux control

Let us now assume that the number of components in the mixture is three since

$$u_w \equiv 0,$$

thus, unlike previous multiphase models in a related context (see e.g., [19, 37]), but compare also [36], we neglect the interstitial fluid and only take into account the more 'solid' components, namely cancer cells, necrotic matter, and normal tissue, all of which are assumed to be more or less heterogeneously interspersed within the volume of interest. In this Subsection we assume all physical laws from *Subsection 3.1* to hold in full, so that, in particular, the mass conservation law (3.6) holds for each $i \in \{c, m, n\}$. Due to (3.1) and (3.5) we can replace (3.6) for $i = n$ by

$$\nabla \cdot J_{sum} = 0, \tag{3.32}$$

where

$$J_{sum} := \sum_{i \in \{c,m,n\}} J_i.$$

As we have seen previously, system (3.19) is underdetermined. However, if J_{sum} is given, then the system is equivalent to the following matrix equation:

$$\bar{A}(J_c, J_m, J_n)^T = (z_c, z_m, J_{sum})^T, \tag{3.33}$$

where

$$\bar{A} = \begin{pmatrix} -(K_{cm}u_m + K_{cn}u_n) & K_{cm}u_c & K_{cn}u_c \\ K_{cm}u_m & -(K_{cm}u_c + K_{mn}u_n) & K_{mn}u_m \\ 1 & 1 & 1 \end{pmatrix} \tag{3.34}$$

and

$$z_i := -u_i \nabla (u \cdot \tau) + \nabla (u_i \tau_i).$$

One can readily verify that

$$\bar{A}^{-1} = \frac{1}{K_{cm}^2 S_1} \begin{pmatrix} -K_{cm}u_c - K_{mn}(u_m + u_n) & u_c(K_{cn} - K_{cm}) & u_c K_{cm}^2 S_1 \\ u_m(K_{mn} - K_{cm}) & -K_{cm}u_m - K_{cn}(u_c + u_n) & u_m K_{cm}^2 S_1 \\ K_{cm}(u_c + u_m) + K_{mn}u_n & K_{cm}(u_c + u_m) + K_{cn}u_n & u_n K_{cm}^2 S_1 \end{pmatrix}, \tag{3.35}$$

where

$$S_1 := \frac{1}{K_{cm}^2}(K_{cm}K_{cn}u_c + K_{cm}K_{mn}u_m + K_{cn}K_{mn}u_n). \tag{3.36}$$

Using (3.5), we can rewrite (3.35) as

$$\bar{A}^{-1} = \frac{1}{K_{cm}^2 S_1} \begin{pmatrix} u_c(K_{mn} - K_{cm}) - K_{mn} & u_c(K_{cn} - K_{cm}) & u_c K_{cm}^2 S_1 \\ u_m(K_{mn} - K_{cm}) & u_m(K_{cn} - K_{cm}) - K_{cn} & u_m K_{cm}^2 S_1 \\ u_n(K_{mn} - K_{cm}) + K_{cm} & u_n(K_{cn} - K_{cm}) + K_{cm} & u_n K_{cm}^2 S_1 \end{pmatrix}$$

$$= \frac{1}{K_{cm}^2 S_1}(u(B_1, B_2, K_{cm}^2 S_1) + (b_1, b_2, (0, 0, 0)^T)), \tag{3.37}$$

where

$$(B_1, B_2) := (K_{mn} - K_{cm}, K_{cn} - K_{cm}), \tag{3.38}$$

$$(b_1, b_2) := \begin{pmatrix} -K_{mn} & 0 \\ 0 & -K_{cn} \\ K_{cm} & K_{cm} \end{pmatrix}. \tag{3.39}$$

Resolving (3.33) with respect to J_i's and using (3.37), we get

$$
\begin{aligned}
(J_c, J_m, J_n) &= \frac{1}{K_{cm}^2 S_1} \left(\left(u \left(B_1, B_2, K_{cm}^2 S_1 \right) + \left(b_1, b_2, (0,0,0)^T \right) \right) (z_c, z_m, J_{sum})^T \right)^T \\
&= \frac{1}{K_{cm}^2 S_1} \left(z_c (B_1 u + b_1)^T + z_m (B_2 u + b_2)^T \right) + J_{sum} u^T.
\end{aligned} \tag{3.40}
$$

Combining (3.38)–(3.40), we obtain

$$
\begin{aligned}
-J_c &= \frac{1}{K_{cm}^2 S_1} \left((K_{cm} u_c + K_{mn}(1 - u_c)) z_c + (K_{cm} - K_{cn}) u_c z_m \right) - J_{sum} u_c \\
&= \frac{1}{K_{cm}^2 S_1} \left((K_{cm} u_c + K_{mn}(1 - u_c))(-u_c \nabla(u \cdot \tau) + \nabla(u_c \tau_c)) \right. \\
&\quad \left. + (K_{cm} - K_{cn}) u_c (-u_m \nabla(u \cdot \tau) + \nabla(u_m \tau_m)) \right) - J_{sum} u_c
\end{aligned} \tag{3.41}
$$

and

$$
\begin{aligned}
-J_m &= \frac{1}{K_{cm}^2 S_1} \left((K_{cm} - K_{mn}) u_m z_c + (K_{cm} u_m + K_{cn}(1 - u_m)) z_m \right) - J_{sum} u_m \\
&= \frac{1}{K_{cm}^2 S_1} \left((K_{cm} - K_{mn}) u_m (-u_c \nabla(u \cdot \tau) + \nabla(u_c \tau_c)) \right. \\
&\quad \left. + (K_{cm} u_m + K_{cn}(1 - u_m))(-u_m \nabla(u \cdot \tau) + \nabla(u_m \tau_m)) \right) - J_{sum} u_m.
\end{aligned} \tag{3.42}
$$

Recalling that $\tau_n = 0$ due to (3.2), we conclude from (3.41)–(3.42) that

$$
\begin{aligned}
-J_c + J_{sum} u_c &= \frac{1}{K_{cm}^2 S_1} (K_{cm} u_c + K_{mn}(1 - u_c))((1 - u_c) \nabla(u_c \tau_c) - u_c \nabla(u_m \tau_m)) \\
&\quad + \frac{1}{K_{cm}^2 S_1} (K_{cm} - K_{cn}) u_c (-u_m \nabla(u_c \tau_c) + (1 - u_m) \nabla(u_m \tau_m)) \\
&= \frac{1}{K_{cm}^2 S_1} \left((K_{cm} u_c + K_{mn}(1 - u_c))(1 - u_c) - (K_{cm} - K_{cn}) u_c u_m \right) \nabla(u_c \tau_c) \\
&\quad + \frac{1}{K_{cm}^2 S_1} \left(-(K_{cm} u_c + K_{mn}(1 - u_c)) u_c + (K_{cm} - K_{cn}) u_c (1 - u_m) \right) \nabla(u_m \tau_m). \tag{3.43}
\end{aligned}
$$

and, similarly,

$$
-J_m + J_{sum} u_m = \frac{1}{K_{cm}^2 S_1} \left(-(K_{cm} u_m + K_{cn}(1 - u_m)) u_m + (K_{cm} - K_{mn}) u_m (1 - u_c) \right) \nabla(u_c \tau_c)
$$

$$+ \frac{1}{K_{cm}^2 S_1}\left((K_{cm}u_m + K_{cn}(1-u_m))(1-u_m) - (K_{cm}-K_{mn})u_c u_m\right)\nabla(u_m\tau_m). \quad (3.44)$$

Set

$$D_{cc} := (K_{cm}u_c + K_{mn}(1-u_c))(1-u_c) + (K_{cn}-K_{cm})u_c u_m, \quad (3.45)$$

$$D_{cm} := -(K_{cm}u_c + K_{mn}(1-u_c))u_c - (K_{cn}-K_{cm})u_c(1-u_m), \quad (3.46)$$

$$D_{mc} := -(K_{cm}u_m + K_{cn}(1-u_m))u_m - (K_{mn}-K_{cm})u_m(1-u_c), \quad (3.47)$$

$$D_{mm} := (K_{cm}u_m + K_{cn}(1-u_m))(1-u_m) + (K_{mn}-K_{cm})u_c u_m. \quad (3.48)$$

Then (3.43) and (3.44) take the form

$$-J_c = \frac{1}{K_{cm}^2 S_1}D_{cc}\nabla(u_c\tau_c) + \frac{1}{K_{cm}^2 S_1}D_{cm}\nabla(u_m\tau_m) - J_{sum}u_c, \quad (3.49)$$

$$-J_m = \frac{1}{K_{cm}^2 S_1}D_{mc}\nabla(u_c\tau_c) + \frac{1}{K_{cm}^2 S_1}D_{mm}\nabla(u_m\tau_m) - J_{sum}u_m. \quad (3.50)$$

Finally, combining (3.2)–(3.6), (3.32), (3.49), and (3.50) we arrive at the system

$$\partial_t u_c = \nabla \cdot \left(\frac{D_{cc}}{K_{cm}^2 S_1}(u_c,u_m)\nabla(u_c\tau_c(u_c,h)) + \frac{D_{cm}}{K_{cm}^2 S_1}(u_c,u_m)\nabla(u_m\tau_m(u_c,u_m)) - J_{sum}u_c\right)$$
$$+ f_c(u_c,u_m,h), \quad (3.51a)$$

$$\partial_t u_m = \nabla \cdot \left(\frac{D_{mc}}{K_{cm}^2 S_1}(u_c,u_m)\nabla(u_c\tau_c(u_c,h)) + \frac{D_{mm}}{K_{cm}^2 S_1}(u_c,u_m)\nabla(u_m\tau_m(u_c,u_m)) - J_{sum}u_m\right)$$
$$+ f_m(u_c,u_m,h), \quad (3.51b)$$

$$u_n := 1 - u_c - u_m, \quad (3.51c)$$

$$\nabla \cdot J_{sum} = 0. \quad (3.51d)$$

Our construction guarantees that u_n satisfies an equation similar to (3.51a) and (3.51b):

$$\partial_t u_n = \nabla \cdot \left(\frac{D_{wc}}{K_{cm}^2 S_1}(u_c,u_m)\nabla(u_c\tau_c(u_c,u_m,h)) + \frac{D_{wm}}{K_{cm}^2 S_1}(u_c,u_m)\nabla(u_m\tau_m(u_c,u_m,h)) - J_{sum}u_n\right)$$
$$+ f_w(u_c,u_m,h), \quad (3.52)$$

where

$$D_{wc} := -(D_{cc} + D_{mc}),$$
$$D_{wm} := -(D_{cm} + D_{mm}),$$

and

$$D_{wc} = D_{wm} = 0 \qquad \text{for all } u \text{ such that } u_c + u_m = 1.$$

This a priori ensures that $u_n \geqslant 0$ is satisfied if the solution components are smooth.

Remark 3.4. Model (3.51) is a generalisation of the model derived in [19]. Unlike that work we require neither the constants K_{ij} to be equal nor the space dimension N to be one.

Remark 3.5. Our allowing the tissues to be displaced (thus giving up the hypothesis of their immovability) led to nonlinear diffusion and drift in (3.51b) (or, for that matter, in (3.52)). This might seem unusual, as most reaction-difusion-transport systems describing cell motility in tissues assume the latter fixed and use ODEs for their evolution. We emphasize that the obtained terms do not state a self-driven motion of these components, but rather the effect of population- and biochemical pressure exerted thereon.

Remark 3.6. To close model (3.51), one needs to choose some divergence-free J_{sum}. In dimension one and for no-flux boundary conditions $J_{sum} \equiv 0$ is the only option. In higher dimensions J_{sum} can be a curl field (in $3D$) or, more generally in N dimensions (cf. [3]), an exterior product of gradients: $J_{sum} = \nabla\gamma_1 \wedge \nabla\gamma_2 \wedge \cdots \wedge \nabla\gamma_{N-1}$. In the physically relevant $3D$ case this means that $J_{sum} = \nabla\gamma_1 \times \nabla\gamma_2$, thus there exist some scalar quantities γ_1, γ_2 (e.g., densities/volume fractions/concentrations) such that the total flux is orthogonal to each of their gradients, or, put in another way, J_{sum} is tangential to a curve which lies in the intersection of the surfaces described by γ_1 and γ_2. This would mean that the total flux is following a direction which is equally biased by those two species. The solenoidality of J_{sum} is a reasonable assumption in view of our previous requirement that there were no sources or sinks of material, either.

Diffusion matrix   Without loss of generality we assume that

$$K_{mn} \geqslant K_{cn} \geqslant K_{cm} > 0. \tag{3.53}$$

One readily verifies that

$$\frac{1}{K_{cm}^2 S_1} \begin{pmatrix} D_{cc} & D_{cm} \\ D_{mc} & D_{mm} \end{pmatrix} = \frac{S_2}{K_{cm}S_1} \begin{pmatrix} 1 - u_c - \frac{u_n}{S_2}\varepsilon_c & -u_c \\ -u_m & 1 - u_m - \frac{u_n}{S_2}\varepsilon_m \end{pmatrix}, \tag{3.54}$$

where

$$\varepsilon_c := \frac{K_{cn}}{K_{cm}} - 1, \qquad \varepsilon_m := \frac{K_{mn}}{K_{cm}} - 1, \tag{3.55}$$

$$S_1 := (1 + \varepsilon_c)u_c + (1 + \varepsilon_m)u_m + (1 + \varepsilon_c)(1 + \varepsilon_m)(1 - u_c - u_m), \tag{3.56}$$

$$S_2 := 1 + \varepsilon_c(1 - u_m) + \varepsilon_m(1 - u_c). \tag{3.57}$$

Due to assumptions (3.53) we have for $0 \leqslant u_c, u_m, u_c + u_m \leqslant 1$ that

$$D_{cc}, D_{mm} \geqslant 0, \qquad D_{cm}, D_{mc} \leqslant 0,$$
$$0 \leqslant \varepsilon_c \leqslant \varepsilon_m,$$
$$S_1 \in [1 + \varepsilon_c, (1 + \varepsilon_c)(1 + \varepsilon_m)], \tag{3.58}$$
$$S_2 \in [1 + \varepsilon_c, 1 + \varepsilon_1 + \varepsilon_m]. \tag{3.59}$$

In particular, for small ε_i matrix (3.54) can be regarded as a perturbation of matrix

$$\frac{1}{K_{cm}} \begin{pmatrix} 1 - u_c & -u_c \\ -u_m & 1 - u_m \end{pmatrix}$$

corresponding to

$$\varepsilon_c = \varepsilon_m = 0,$$

i.e., to

$$K_{mn} = K_{cn} = K_{cm}.$$

This case was addressed in [22]. Further, we compute

$$\begin{pmatrix} \partial_{u_c}(u_c\tau_c) & \partial_{u_m}(u_c\tau_c) & \partial_h(u_c\tau_c) \\ \partial_{u_c}(u_m\tau_m) & \partial_{u_m}(u_m\tau_m) & \partial_h(u_m\tau_m) \end{pmatrix} = \begin{pmatrix} 2\alpha_c u_c & 0 & u_c g' \\ \theta\alpha_m u_m^2 & 2\alpha_m(1 + \theta u_c)u_m & 0 \end{pmatrix}. \tag{3.60}$$

Overall, the diffusion matrix of equations (3.51a) and (3.51b) takes the form

$$\frac{S_2}{K_{cm}S_1} \begin{pmatrix} 1 - u_c - \frac{u_n}{S_2}\varepsilon_c & -u_c \\ -u_m & 1 - u_m - \frac{u_n}{S_2}\varepsilon_m \end{pmatrix} \begin{pmatrix} 2\alpha_c u_c & 0 & u_c g' \\ \theta\alpha_m u_m^2 & 2\alpha_m(1 + \theta u_c)u_m & 0 \end{pmatrix}. \tag{3.61}$$

The complete diffusion matrix of (3.51a), (3.51b), and (3.11) includes the third line

$$(0, 0, D_h). \tag{3.62}$$

4. Existence of weak solutions to (3.51a)–(3.51c), (3.11)

In this section we use the method that was presented in [21] in order to establish an existence result for our cross diffusion system (3.51a)–(3.51c), (3.11). The key to applying the method is finding a suitable so-called entropy density. Motivated by the study in [22], where the case of equal K_{ij}'s and no acidity was treated, we consider the following entropy density:

$$E : \mathcal{D} \to \mathbb{R}, \quad \mathcal{D} := \mathcal{D}_{cm} \times (0, \infty), \quad \mathcal{D}_{cm} := \{(u_c, u_m) \in (0, 1)^2 : \quad u_c + u_m < 1\}, \tag{4.1a}$$

$$E(u_c, u_m, h) := L(u_c, u_m) + \frac{a}{2}h^2, \tag{4.1b}$$

$$L(u_c, u_m) := u_c(\ln(u_c) - 1) + u_m(\ln(u_m) - 1) + u_n(\ln(u_n) - 1), \tag{4.1c}$$

$$u_n := 1 - (u_c + u_m). \tag{4.1d}$$

Here L is the well-known logarithmic entropy and $a > 0$ is a sufficiently large constant yet to be fixed. For the subsequent computations we need the matrix of second-order partial derivatives of E:

$$D^2 E(u_c, u_m, h) = \begin{pmatrix} \frac{1}{u_n}\frac{1-u_m}{u_c} & \frac{1}{u_n} & 0 \\ \frac{1}{u_n} & \frac{1}{u_n}\frac{1-u_c}{u_m} & 0 \\ 0 & 0 & a \end{pmatrix}. \tag{4.2}$$

In order to be able to apply the method from [21], we need to ensure positive (semi-)definiteness of matrix $(D^2E)M$ in $\mathcal{D}$ where M is the diffusion matrix of (3.51a), (3.51b), and (3.11). In this Subsection we verify this property for the parameter values satisfying the following conditions:

$$0 < \min_{y\in[0,1]} \left(4\alpha_m\left(1 + \varepsilon_c(1-y)\right)\right)\left(4\alpha_c\left(1 + \varepsilon_m\right) - 2\theta\alpha_m y^2\varepsilon_m\right) - \alpha_m^2 y^2 \left(\theta\left(1 + \varepsilon_c(1-y)\right) - 2\varepsilon_m\right)^2 \tag{4.3}$$

and

$$0 < \min_{y \in [0,1]} \left(4\alpha_m \left(1 + \theta y \right) \left(1 + \varepsilon_c y \right) \left(4\alpha_c \left(1 + \varepsilon_m (1 - y) \right) - 2\theta\alpha_m (1 - y)^2 \varepsilon_m \right) \right.$$

$$\left. - \left(-2\alpha_c y \varepsilon_c + \theta\alpha_m (1 - y) \left(1 + \varepsilon_c y \right) - 2\alpha_m (1 - y) \left(1 + \theta y \right) \varepsilon_m \right)^2 \right), \tag{4.4}$$

where ε_c and ε_m are constants defined in (3.55).

Remark 4.1. Since both functions which need to be minimised in (4.3) and (4.4) are fourth degree polynomials in y, these conditions can be readily checked numerically for a set of given parameters.

Lemma 4.2 (Uniform ellipticity). *Let (4.3) and (4.4) hold. Let E be as defined in (4.1). Then there exist some constants $a > 0$ and $0 < C_1 \leqslant C_2 < \infty$, such that:*

$$C_1 |y|^2 \leqslant y^T ((D^2 E) M)(u_c, u_m, h) y \leqslant C_2 |y|^2 \qquad \text{for all } (u_c, u_m, h) \in \mathcal{D}, \ y \in \mathbb{R}^3. \tag{4.5}$$

Proof. To begin with, we compute

$$S_2 \begin{pmatrix} \partial^2_{u_c u_c} E & \partial^2_{u_c u_m} E \\ \partial^2_{u_c u_m} E & \partial^2_{u_m u_m} E \end{pmatrix} \begin{pmatrix} 1 - u_c - \frac{u_n}{S_2} \varepsilon_c & -u_c \\ -u_m & 1 - u_m - \frac{u_n}{S_2} \varepsilon_m \end{pmatrix} = \begin{pmatrix} \frac{1}{u_c} \beta_c & -\varepsilon_m \\ -\varepsilon_c & \frac{1}{u_m} \beta_m \end{pmatrix}, \tag{4.6}$$

where

$$\beta_c := 1 + \varepsilon_m (1 - u_c), \qquad \beta_m := 1 + \varepsilon_c (1 - u_m),$$

so that

$$\beta_c \in [1, 1 + \varepsilon_m], \qquad \beta_m \in [1, 1 + \varepsilon_c]. \tag{4.7}$$

Combining (3.61), (3.62), (4.2), and (4.6), we obtain (arguments of functions are omitted)

$$(D^2 E) M = \frac{1}{K_{cm} S_1} \begin{pmatrix} 2\alpha_c \beta_c - \theta\alpha_m u_m^2 \varepsilon_m & -2\alpha_m (1 + \theta u_c) u_m \varepsilon_m & \beta_c g' \\ -2\alpha_c u_c \varepsilon_c + \theta\alpha_m u_m \beta_m & 2\alpha_m (1 + \theta u_c) \beta_m & -u_c \varepsilon_c g' \\ 0 & 0 & a D_h S_2 \end{pmatrix}. \tag{4.8}$$

We introduce the symmetric matrix

$$P := (D^2 E) M + ((D^2 E) M)^T = \frac{1}{K_{cm} S_1} \begin{pmatrix} \tilde{P} & \begin{matrix} \beta_c g' \\ -u_c \varepsilon_c g' \end{matrix} \\ \begin{matrix} \beta_c g' & -u_c \varepsilon_c g' \end{matrix} & 2 a D_h S_2 \end{pmatrix},$$

where

$$\tilde{P} := \begin{pmatrix} 4\alpha_c \beta_c - 2\theta\alpha_m u_m^2 \varepsilon_m & -2\alpha_c u_c \varepsilon_c + \theta\alpha_m u_m \beta_m - 2\alpha_m (1 + \theta u_c) u_m \varepsilon_m \\ -2\alpha_c u_c \varepsilon_c + \theta\alpha_m u_m \beta_m - 2\alpha_m (1 + \theta u_c) u_m \varepsilon_m & 4\alpha_m (1 + \theta u_c) \beta_m \end{pmatrix}. \tag{4.9}$$

Next, we study $\det(\tilde{P})$ in $\mathcal{D}_{cm}$. We compute

$$d_P := \det(\tilde{P})$$

$$=4\alpha_m(1+\theta u_c)\beta_m(4\alpha_c\beta_c - 2\theta\alpha_m u_m^2\varepsilon_m) - (-2\alpha_c u_c\varepsilon_c + \theta\alpha_m u_m\beta_m - 2\alpha_m(1+\theta u_c)u_m\varepsilon_m)^2$$

$$=4\alpha_m\left(1+\theta u_c\right)\left(1+\varepsilon_c(1-u_m)\right)\left(4\alpha_c\left(1+\varepsilon_m(1-u_c)\right) - 2\theta\alpha_m u_m^2\varepsilon_m\right)$$

$$- \left(-2\alpha_c u_c\varepsilon_c + \theta\alpha_m u_m\left(1+\varepsilon_c(1-u_m)\right) - 2\alpha_m\left(1+\theta u_c\right)u_m\varepsilon_m\right)^2.$$

Observe that d_P is quadratic with respect to u_c, and the coefficient of u_c^2 is negative. Consequently, d_P cannot attain its minimum inside $\mathcal{D}_{cm} \cup ((0,1) \times \{0\})$. It remains to ensure that d_P is positive on the sets $\{0\} \times [0,1]$ and $\{(u_c, u_m) \in (0,1] \times [0,1) : u_c + u_m = 1\}$. This the case if

$$\min_{y\in[0,1]} d_P(0,y)$$

$$= \min_{y\in[0,1]} \left(4\alpha_m\left(1+\varepsilon_c(1-y)\right)\left(4\alpha_c\left(1+\varepsilon_m\right) - 2\theta\alpha_m y^2\varepsilon_m\right) - \alpha_m^2 y^2\left(\theta\left(1+\varepsilon_c(1-y)\right) - 2\varepsilon_m\right)^2\right)$$

$$>0 \tag{4.10}$$

and

$$\min_{y\in[0,1]} d_P(y, 1-y) = \min_{y\in[0,1]} \left(4\alpha_m\left(1+\theta y\right)\left(1+\varepsilon_c y\right)\left(4\alpha_c\left(1+\varepsilon_m(1-y)\right) - 2\theta\alpha_m(1-y)^2\varepsilon_m\right)\right.$$

$$\left. - \left(-2\alpha_c y\varepsilon_c + \theta\alpha_m(1-y)\left(1+\varepsilon_c y\right) - 2\alpha_m\left(1-y\right)\left(1+\theta y\right)\varepsilon_m\right)^2\right)$$

$$>0. \tag{4.11}$$

By Sylvester's criterion, P is positive definite if and only if $\tilde{P}$ is positive definite and $\det(P) > 0$. Due to (3.58)–(3.59), (4.7), and g Lipschitz all functions involved in (4.9) are bounded and functions $S_1, S_2, \beta_c, \beta_m$ have positive lower bounds in $\mathcal{D}$. In particular, $\tilde{P}_{22} \geqslant 2\alpha_m > 0$, so that $\tilde{P}$ is positive definite if and only if $\det(\tilde{P}) > 0$. Further, we have

$$\det(P) = aD_h S_2 \det(\tilde{P}) + \varphi$$

$$\geqslant aD_h \det(\tilde{P}) + \varphi,$$

where $\varphi : \overline{\mathcal{D}} \to \mathbb{R}$ is a bounded function (recall that g is Lipschitz). Thus, for sufficiently large a, $\det(P) > 0$ holds provided that $\det(\tilde{P}) > 0$. Altogether, we conclude that conditions (4.10) and (4.11) imply that matrix P is positive for all triples in $\overline{\mathcal{D}}$. Assuming these conditions to be satisfied, let $\lambda(P)$ denote an eigenvalue of P. Then

$$\frac{\det(P)}{\text{trace}^2(P)} \leqslant \lambda(P) \leqslant \text{trace}(P).$$

In $\overline{\mathcal{D}}$, functions $\text{trace}(P)$ and $\det(P)$ are bounded from above and from below, respectively, by some positive constants. Hence, we have positive lower and upper bounds for the eigenvalues of P. □

Now we are ready to state our existence result.

Theorem 4.3. *Let $0 < K_{cm} \leqslant K_{cn} \leqslant K_{mn}$ and $\alpha_c, \alpha_m, \theta, h_{max}, \chi > 0$ be some constants which satisfy (3.55), (4.3), and (4.4). Let coefficients τ_c and τ_m be as defined in (3.3) and (3.4) and let Lipschitz functions $f_c, f_m, f_h : \overline{\mathcal{D}} \to \mathbb{R}$, with domain $\mathcal{D}$ as in (4.1a), be such that*

$$f_i \geqslant 0 \qquad \text{for } u_i = 0, \quad i \in \{c, m\}, \tag{4.12a}$$

$$f_c + f_n \leqslant 0 \qquad for\ u_c + u_m = 1, \tag{4.12b}$$

$$f_h \geqslant 0 \qquad for\ h = 0. \tag{4.12c}$$

Then for every given $J_{sum} \in L^2_{loc}([0, \infty); (L^2(\Omega))^n)$ and $(u_{c0}, u_{m0}, h) \in (L^\infty(\Omega))^2 \times L^2(\Omega)$ such that $(u_{c0}, u_{m0}, h)(x) \in \overline{\mathcal{D}}$ for a.a. $x \in \Omega$ there exists a weak solution $(u_c, u_m, h) : [0, \infty) \times \Omega \to \overline{\mathcal{D}}$ to system (3.51a)–(3.51c), (3.11) under no-flux boundary conditions. This means that:

$$(u_c, u_m, h) \in L^2_{loc}([0, \infty); (H^1(\Omega))^3), \quad \partial_t(u_c, u_m, h) \in L^2_{loc}([0, \infty); ((H^1(\Omega))^3)'), \tag{4.13}$$

$$\langle \partial_t u_c, \varphi \rangle = -\int_\Omega \left(\frac{D_{cc}}{K^2_{cm}S_1}(u_c, u_m)\nabla(u_c\tau_c(u_c, h)) + \frac{D_{cm}}{K^2_{cm}S_1}(u_c, u_m)\nabla(u_m\tau_m(u_c, u_m)) - J_{sum}u_c \right) \cdot \nabla\varphi\, dx$$
$$+ \int_\Omega \varphi f_c(u_c, u_n, h)\, dx, \tag{4.14a}$$

$$\langle \partial_t u_m, \varphi \rangle = -\int_\Omega \left(\frac{D_{mc}}{K^2_{cm}S_1}(u_c, u_m)\nabla(u_c\tau_c(u_c, h)) + \frac{D_{mm}}{K^2_{cm}S_1}(u_c, u_m)\nabla(u_m\tau_m(u_c, u_m)) - J_{sum}u_m \right) \cdot \nabla\varphi\, dx$$
$$+ \int_\Omega \varphi f_m(u_c, u_m, h)\, dx, \tag{4.14b}$$

$$\langle \partial_t h, \varphi \rangle = -\int_\Omega D_h\nabla h \cdot \nabla\varphi\, dx + \int_\Omega \varphi f_h(u_c, u_m, h)\, dx \tag{4.14c}$$

a.e. in $(0, \infty)$ for all $\varphi \in H^1(\Omega)^3$, and the initial conditions for each variable are satisfied in $L^2(\Omega)$-sense.

Remark 4.4. Using the assumptions on the coefficients of system (3.51a)–(3.51c), (3.11), one readily verifies that if (u_c, u_m, h) satisfies (4.13) and $(u_c, u_m, h) \in \mathcal{D}$ a.e., then the gradients $\nabla(u_c\tau_c(u_c, u_m))$ and $\nabla(u_m\tau_m(u_c, u_m))$ as well as the fluxes in (4.14a) and (4.14b) belong to $L^2_{loc}([0, \infty); (L^2(\Omega))^N)$.

Proof of Theorem 4.3 (sketch). We rely on the theory of weak solvability for cross diffusion systems which was developed in [21]. We recall that the main tool of the method in [21] is a suitable entropy density. Here we use function $E : \mathcal{D} \to \mathbb{R}$ previously defined in (4.1). This function is the sum of the standard logarithmic entropy L for variables u_1 and u_2 and the quadratic ah^2. Combining the corresponding properties of the logarithmic entropy and our previous calculations in this section, we obtain:

H1: $E \in C^2(\mathcal{D})$ and is convex and bounded below by

$$\min_{\mathcal{D}} E = E\left(\frac{1}{3}, \frac{1}{3}, \frac{1}{3}, 0\right).$$

The derivative

$$DE : \mathcal{D} \to \mathbb{R}^3, \qquad DE = (\ln(u_c) - \ln(u_n), \ln(u_m) - \ln(u_n), ah) \tag{4.15}$$

is invertible, the inverse being

$$(DE)^{(-1)}(z_1, z_2, z_3) = \left(\frac{e^{z_1}}{1 + e^{z_1} + e^{z_2}}, \frac{e^{z_2}}{1 + e^{z_1} + e^{z_2}}, \frac{1}{a}z_3 \right).$$

H2': For sufficiently large a, left multiplying the diffusion matrix M by $D^2 E$ yields a uniformly positive definite matrix (see *Lemma 4.2*).

H2": The diffusion matrix M is uniformly bounded in $\mathcal{D}$ (compare (3.61) and (3.62), recall that g is Lipschitz).

H3: M and f_i, $i \in \{c, m, h\}$, are continuous mappings and there exists a constant C_3 such that

$$DE \cdot (f_c, f_m, f_h) \leqslant C_3 \left(1 + E - \min_{\mathcal{D}} E \right) \qquad \text{in } \mathcal{D}. \tag{4.16}$$

Estimate (4.16) is a standard consequence of the assumptions (4.12). Indeed, since $z \mapsto z \ln z$ is negative and bounded below in $(0, 1)$, the part originating from the logarithmic entropy satisfies

$$
\begin{aligned}
(\partial_{u_c} L, \partial_{u_m} L) \cdot (f_c, f_m) = & f_c \ln(u_c) + f_m \ln(u_m) + (-f_c - f_m) \ln(u_n) \\
\leqslant & - \|\nabla f_c\|_{L^\infty(\mathcal{D})} u_c \ln(u_c) - \|\nabla f_m\|_{L^\infty(\mathcal{D})} u_m \ln(u_m) \\
& - \left(\|\nabla f_c\|_{L^\infty(\mathcal{D})} + \|\nabla f_m\|_{L^\infty(\mathcal{D})} \right) (1 - (u_c + u_m)) \ln(1 - (u_c + u_m)) \\
\leqslant & C_4 \qquad \text{in } \mathcal{D}
\end{aligned}
\tag{4.17}
$$

for some constant $C_4 > 0$. Further, since f_h is Lipschitz, we also have

$$\partial_h E f_h \leqslant C_5 (1 + ah^2) \qquad \text{in } \mathcal{D} \tag{4.18}$$

for some constant $C_5 > 0$. Adding (4.17) and (4.18) together, we obtain

$$
\begin{aligned}
DE \cdot (f_c, f_m, f_h) \leqslant & C_6 (1 + ah^2) \\
\leqslant & C_3 \left(1 + L - \min_{\mathcal{D}} L + ah^2 \right) \\
= & C_3 \left(1 + E - \min_{\mathcal{D}} E \right) \qquad \text{in } \mathcal{D}
\end{aligned}
$$

since obviously $\min E = \min L$.

The main result of [21], Theorem 2 on existence of bounded weak solutions, cannot be directly applied in our case for two reasons: firstly, apart from diffusion and reaction, equations for u_c and u_m also involve transport in the direction of a given vector-valued function J_{sum}; secondly, the domain $\mathcal{D}$ is not bounded. Were it not for these differences, the above properties H1–H3 would correspond to the hypotheses H1–H3 in [21]. Still, the proof of existence of weak solutions can be carried out very similar to the proofs presented in [21]. The latter go through the following steps: approximation of the time derivative using the implicit Euler scheme, regularisation of the diffusion operator by adding a higher order differential operator such as $\epsilon(I + (-\Delta)^m)$ for $m > N/2$ and small ϵ, solving the linearised approximation problem using the Lax-Milgram lemma, solving the nonlinear approximation problem using the Leray-Schauder theorem, establishing uniform estimates, and, finally, using the compactness method in order to pass to the limit and solve the original problem. Our case can be handled in the very same way. Indeed, on the one hand the linear transport along J_{sum} is subordinate to diffusion, so that it, e.g., does not hinder the derivation of estimates. On the other hand even though $\mathcal{D}$ is not bounded, we actually know that for bounded h_0 the h-component of a solution is a priori bounded on all finite time cylinders. This is a consequence of the standard theory of semilinear parabolic PDEs. General

$h_0 \in L^2(\Omega)$ can be regularised and a corresponding solution obtained by means of yet one more limit procedure.

We omit further details and refer the interested reader to [21] where the complete proofs for very similar cases can be found. □

5. Numerical study

We perform numerical simulations of the system (3.51) supplemented with the PDE (3.11) for the evolution of proton concentration h, endowed with no-flux boundary conditions. For simplicity we choose $J_{sum} = 0$. We also perform a nondimensionalisation of the model and use it in our simulations (for its concrete form and for the employed parameters refer to the Appendix). The initial conditions are as follows:

$$u_c(0, \mathbf{x}) = 0.05 \left(e^{\frac{-(x-500)^2-(y-500)^2}{2(25)^2}} + e^{\frac{-(x-600)^2-(y-500)^2}{2(20)^2}} + e^{\frac{-(x-300)^2-(y-400)^2}{2(10)^2}} \right), \tag{5.1a}$$

$$h(0, \mathbf{x}) = 10^{-7} e^{\frac{-(x-500)^2-(y-500)^2}{2(15)^2}} + 10^{-7} e^{\frac{-(x-600)^2-(y-500)^2}{2(10)^2}} + 10^{-6.4} e^{\frac{-(x-300)^2-(y-400)^2}{2(7.5)^2}}, \tag{5.1b}$$

$$u_n(0, \mathbf{x}) = 0.9 \left(e^{\frac{-(x-500)^2-(y-500)^2}{2(5)^2}} + e^{\frac{-(x-600)^2-(y-500)^2}{2(2)^2}} + e^{\frac{-(x-300)^2-(y-400)^2}{2(1)^2}} \right), \tag{5.1c}$$

$$u_m(0, \mathbf{x}) = 1 - u_c(0, \mathbf{x}) - u_n(0, \mathbf{x}) \quad \text{with} \quad u_m(0, 500, 500) = u_m(0, 600, 500) = u_m(0, 300, 400) = 0. \tag{5.1d}$$

These are illustrated in Figure 1. The problem is set in a square $[0, 1000] \times [0, 1000]$ (in μm), corresponding to the size of large pseudopalisades [5]. For the discretisation we use a method of lines approach. Thereby, the diffusion terms in all involved PDEs are computed by using a standard central difference scheme, while a first order upwind scheme is employed for the advection terms occurring in the equations for glioma and normal tissue. For the acidity equation we discretise time upon using an implicit-explicit (IMEX) method, with forward and backward Euler schemes for the diffusion and reaction terms, respectively. The glioma and normal tissue PDEs are discretised in time by an explicit Euler method.
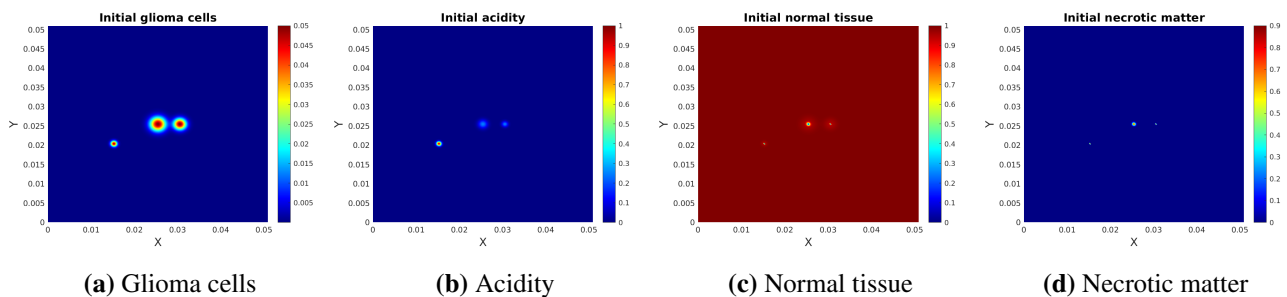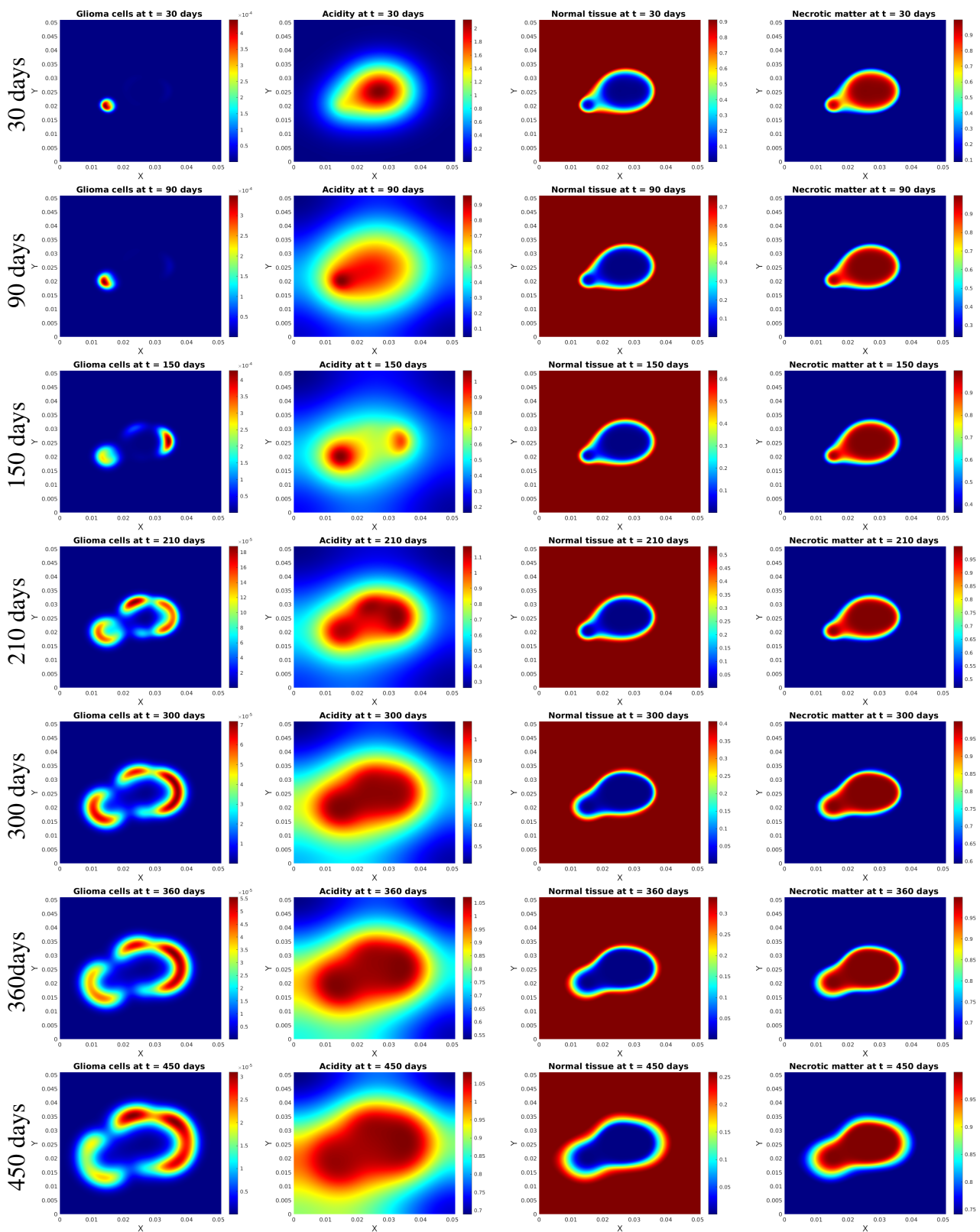

(a) Glioma cells   **(b)** Acidity   **(c)** Normal tissue   **(d)** Necrotic matter

Figure 1. Initial conditions (5.1).

(a) Glioma cells   **(b)** Acidity   **(c)** Normal tissue   **(d)** Necrotic matter

Figure 2. Computed u_c, h, u_m, and u_n from (3.51) and (3.11) with initial conditions (5.1) and with no-flux boundary conditions.

(a) Glioma cells difference **(b)** Acidity difference **(c)** Normal tissue difference **(d)** Necrotic matter difference
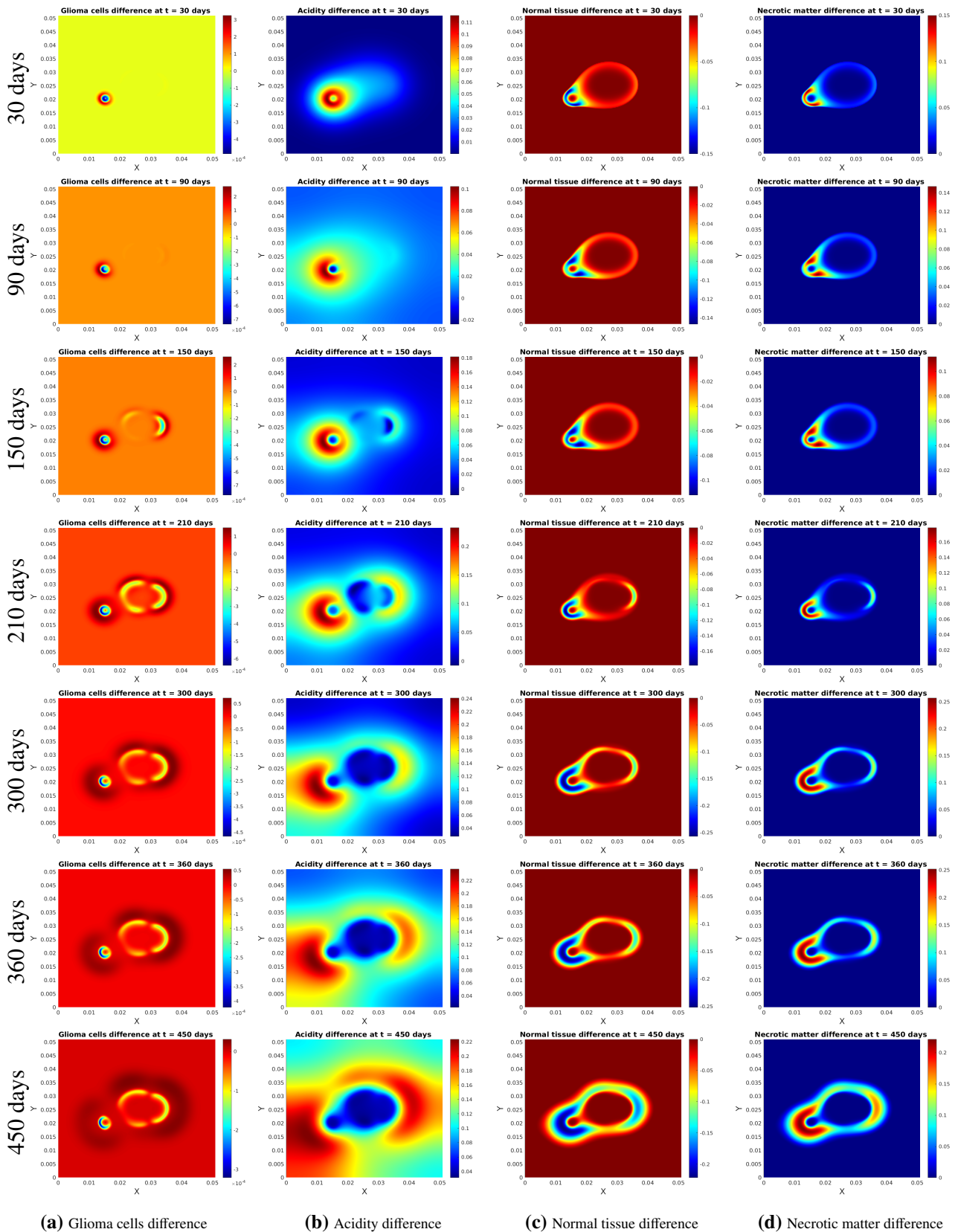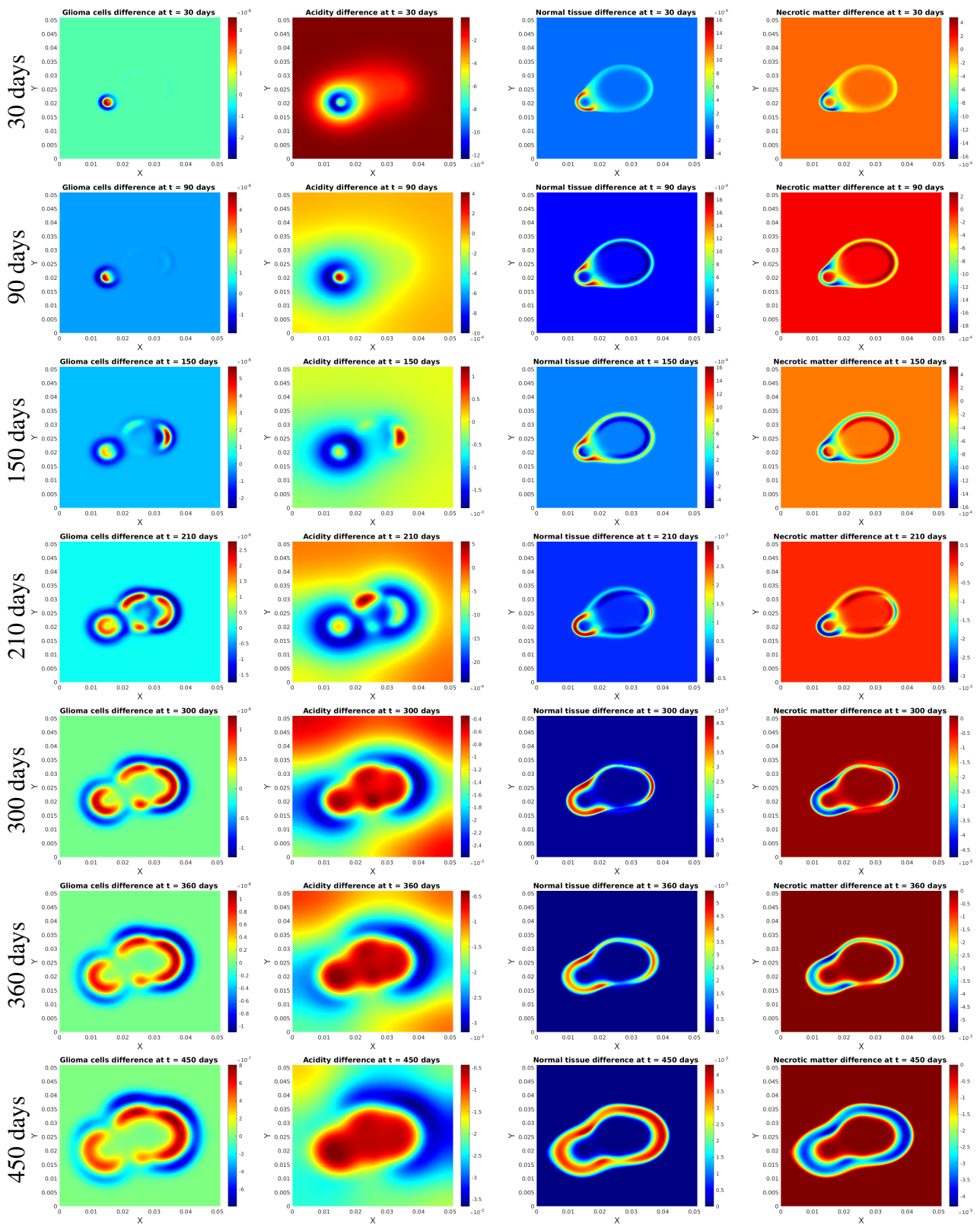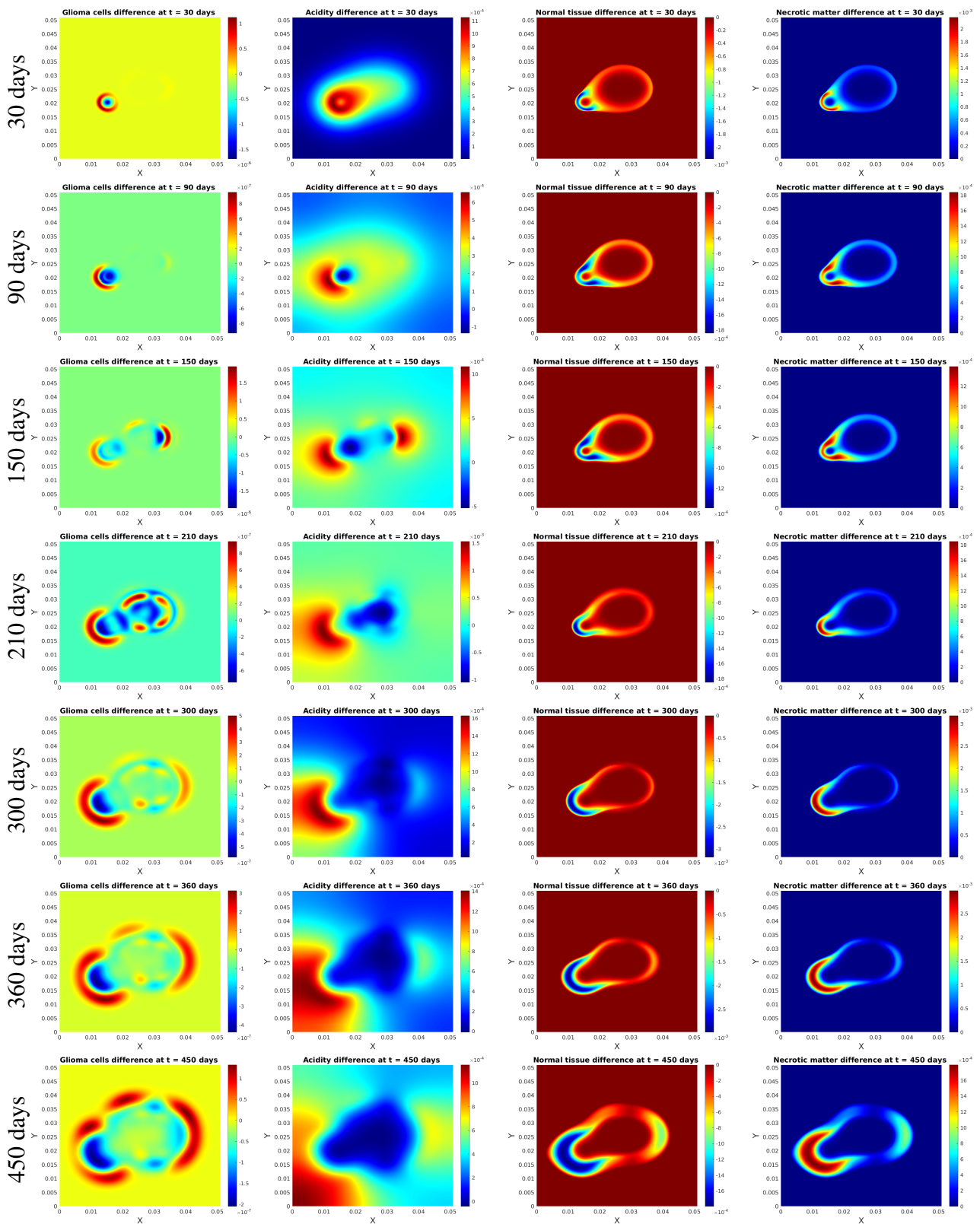
Figure 3. Difference between solution components obtained with $\chi > 0$ and those computed with $\chi = 0$.

(a) Glioma cells difference   **(b)** Acidity difference   **(c)** Normal tissue difference   **(d)** Necrotic matter difference

Figure 4. Difference between solution components obtained with $K_{cm} < K_{mn} < K_{cn}$ and those computed with $K_{cm} = K_{mn} = K_{cn}$, all at the previously lower value K_{cm}.

(a) Glioma cells difference   **(b)** Acidity difference   **(c)** Normal tissue difference   **(d)** Necrotic matter difference

Figure 5. Difference between solution components obtained with $K_{cm} < K_{mn} < K_{cn}$ and those computed with $K_{cm} = K_{mn} = K_{cn}$, all at the previously intermediate value K_{mn}.

Figure 2 shows the computed volume fractions of glioma (first column), normal tissue (3rd column), necrotic matter (last column), and acidity concentration (second column) at several times, in a total time span which is relevant for pseudopalisade formation. The typical garland-like structure of glioma pseudopalisades is clearly visible. The tumor cells encircle a highly acidic and necrotic region, while outwards, beyond the glioma ring, the normal tissue remains non-depleted and the acidity decreases.

To investigate the effect of acidity we compare the previous results with those obtained for $\chi = 0$, i.e., in the absence of additional pressure on glioma cells due to acidosis, recall (3.3). The corresponding plots are shown in Figure 3. The effect of repellent pH-taxis can be seen in the difference between the solution components in two situations (with $\chi > 0$, with pH-taxis and acid-influenced motility, respectively with $\chi = 0$). The pseudopalisades develop faster and get thicker and more extensive in the former case, accompanied by enhanced acidity in the proximity of higher cancer cell densities and enhanced normal tissue depletion inside the ring-shaped structures and around the glioma aggregates, which also triggers a higher volume fraction for the necrotic matter. These observations are in line with those obtained in [26] by another modeling approach: the repellent pH-taxis is not the driving factor of pseudopalisade formation, but it leads to wider such structures.

Finally, we also study the effect of drag coefficients K_{cm}, K_{mn}, K_{cn} in (3.9). Recall that they represent the resistance inferred by the phases in contact when passing over each other. They are contained in the diffusion and drift coefficients of system (3.51). In the computations for Figure 2 we had considered them to be different, more precisely $K_{cm} < K_{mn} < K_{cn}$. This ensured a relatively easy movement of glioma through normal tissue when compared to the shift over necrotic matter of both normal tissue and cancer cells. Now let all these drag coefficients be equal (as was assumed in [19]) and take the previously lowermost value K_{cm}, thus reducing the drag between necrotic matter and the other two phases. The differences between the two cases are plotted in Figure 4 and show in the second case an enhanced outward migration of glioma cells, away from the highly acidic area at the core of the pseudopalisade and with a pronounced suppression of normal cells, and emergence of larger necrotic matter. An opposite effect is noticed when letting $K_{cm} = K_{mn} = K_{cn}$, all at the previously highest value K_{cn}; we do not show here those results (we refer for them to [25]), but rather illustrate in Figure 5 the situation when all drag coefficients equal the previously intermediate value K_{mn}. This means that the drag between cancer cells and normal tissue is increased, while they can easier shift over the necrotic matter. As a consequence, the extent of the pseudopalisades is reduced, but the glioma aggregates in the garland-like structures are larger. This is due not only to the higher drag between cancer cells and normal tissue, but also to the lower K_{cn} value, which ensures that the glioma cells can leave faster than previously the acidic area inside the 'ring'. Around the site where the cancer cells were initially more concentrated the necrosis is reduced and the normal tissue is better preserved.

Acknowledgement

Conflict of interest

The authors declare no conflict of interest.

References

1. J. Alfonso, A. Köhn-Luque, T. Stylianopoulos, F. Feuerhake, A. Deutsch, H. Hatzikirou, Why one-size-fits-all vaso-modulatory interventions fail to control glioma invasion: in silico insights, *Sci. Rep.*, **6** (2016), 37283.

2. R. J. Atkin, R. E. Craine, Continuum theories of mixtures: basic theory and historical development, *The Quarterly Journal of Mechanics and Applied Mathematics*, **29** (1976), 209–244.

3. C. Barbarosie, Representation of divergence-free vector fields, *Q. Appl. Math.*, **69** (2011), 309–316.

4. N. Bellomo, *Modeling complex living systems*, Boston: Birkhäuser, 2008.

5. D. J. Brat, A. A. Castellano-Sanchez, S. B. Hunter, M. Pecot, C. Cohen, E. H. Hammond, et al., Pseudopalisades in glioblastoma are hypoxic, express extracellular matrix proteases, and are formed by an actively migrating cell population, *Cancer Res.*, **64** (2004), 920–927.

6. D. J. Brat, T. B. Mapstone, Malignant glioma physiology: Cellular response to hypoxia and its role in tumor progression, *Ann. Intern. Med.*, **138** (2003), 659–668.

7. C. Breward, H. Byrne, C. Lewis, The role of cell-cell interactions in a two-phase model for avascular tumour growth, *J. Math. Biol.*, **45** (2002), 125–152.

8. H. Byrne, J. King, D. McElwain, L. Preziosi, A two-phase model of solid tumour growth, *Appl. Math. Lett.*, **16** (2003), 567–573.

9. M. Conte, C. Surulescu, Mathematical modeling of glioma invasion: acid- and vasculature mediated go-or-grow dichotomy and the influence of tissue anisotropy, *Appl. Math. Comput.*, **407** (2021), 126305.

10. G. Corbin, A. Klar, C. Surulescu, C. Engwer, M. Wenske, J. Nieto, et al., Modeling glioma invasion with anisotropy- and hypoxia-triggered motility enhancement: From subcellular dynamics to macroscopic pdes with multiple taxis, *Math. Models Methods Appl. Sci.*, **31**, (2021), 177–222.

11. A. Dietrich, N. Kolbe, N. Sfakianakis, C. Surulescu, Multiscale modeling of glioma invasion: from receptor binding to flux-limited macroscopic pdes, 2020, *arXiv:2010.03277*.

12. D. A. Drew, S. L. Passman, *Theory of multicomponent fluids*, New York: Springer, 1999.

13. S. E. Eikenberry, T. Sankar, M. C. Preul, E. J. Kostelich, C. J. Thalhauser, Y. Kuang, Virtual glioblastoma: growth, migration and treatment in a three-dimensional mathematical model, *Cell Prolif.*, **42** (2009), 511–528.

14. C. Engwer, T. Hillen, M. Knappitsch, C. Surulescu, Glioma follow white matter tracts: a multiscale DTI-based model, *J. Math. Biol.*, **71** (2015) ,551–582.

15. C. Engwer, A. Hunt, C. Surulescu, Effective equations for anisotropic glioma spread with proliferation: a multiscale approach and comparisons with previous settings, *Math. Med. Biol.*, **33** (2015), 435–459.

16. C. Engwer, M. Knappitsch, C. Surulescu, A multiscale model for glioma spread including cell-tissue interactions and proliferation, *Math. Biosci. Eng.*, **13** (2016), 443–460.

17. H. Garcke, K. F. Lam, R. Nürnberg, E. Sitka, A multiphase cahn-hilliard-darcy model for tumour growth with necrosis, *Math. Models Methods Appl. Sci.*, **28** (2018), 525–577.

18. A. Hunt, C. Surulescu, A multiscale modeling approach to glioma invasion with therapy, *Vietnam J. Math.*, **45** (2016), 221–240.

19. T. L. Jackson, H. M. Byrne, A mechanical model of tumor encapsulation and transcapsular spread, *Math. Biosci.*, **180** (2002), 307–328.

20. A. F. Jones, H. M. Byrne, J. S. Gibson, J. W. Dold, A mathematical model of the stress induced during avascular tumour growth, *J. Math. Biol.*, **40** (2000), 473–499.

21. A. Jüngel, The boundedness-by-entropy method for cross-diffusion systems, *Nonlinearity*, **28** (2015), 1963–2001.

22. A. Jüngel, I. V. Stelzer, Entropy structure of a cross-diffusion tumor-growth model, *Math. Models Methods Appl. Sci.*, **22** (2012), 1250009.

23. P. Kleihues, F. Soylemezoglu, B. Schäuble, B. W. Scheithauer, P. C. Burger, Histopathology, classification, and grading of gliomas, *Glia*, **15** (1995), 211–221.

24. N. Kolbe, N. Sfakianakis, C. Stinner, C. Surulescu, J. Lenz, Modeling multiple taxis: Tumor invasion with phenotypic heterogeneity, haptotaxis, and unilateral interspecies repellence, *Discrete Contin. Dyn. Syst. Ser. B*, **26** (2021), 443–481.

25. P. Kumar, Mathematical modeling of glioma patterns as a consequence of acidosis and hypoxia, PhD thesis of TU Kaiserslautern, 2021.

26. P. Kumar, J. Li, C. Surulescu, Multiscale modeling of glioma pseudopalisades: contributions from the tumor microenvironment, *J. Math. Biol.*, **82** (2021), 49.

27. P. Kumar, C. Surulescu, A flux-limited model for glioma patterning with hypoxia-induced angiogenesis, *Symmetry*, **12** (2020), 1870.

28. G. Lemon, J. King, Multiphase modelling of cell behaviour on artificial scaffolds: effects of nutrient depletion and spatially nonuniform porosity, *Math. Med. Biol.*, **24** (2007), 57–83.

29. G. R. Martin, R. K. Jain, Noninvasive measurement of interstitial pH profiles in normal and neoplastic tissue using fluorescence ratio imaging microscopy, *Cancer Res.*, **54** (1994), 5670–5674.

30. A. Martínez-González, G. F. Calvo, L. A. Pérez Romasanta, V. M. Pérez-García, Hypoxic cell waves around necrotic cores in glioblastoma: a biomathematical model and its therapeutic implications, *Bull. Math. Biol.*, **74** (2012), 2875–2896.

31. K. J. Painter, T. Hillen, Mathematical modelling of glioma growth: the use of diffusion tensor imaging (DTI) data to predict the anisotropic pathways of cancer invasion, *J. Theor. Biol.*, **323** (2013), 25–39.

32. L. Preziosi, A. Tosin, Multiphase modelling of tumour growth and extracellular matrix interaction: mathematical tools and applications, *J. Math. Biol.*, **58** (2009), 625.

33. L. Preziosi, G. Vitale, A multiphase model of tumor and tissue growth including cell adhesion and plastic reorganization, *Math. Models Methods Appl. Sci.*, **21** (2011), 1901–1932.

34. G. Sciumè, S. Shelton, W. G. Gray, C. T. Miller, F. Hussain, M. Ferrari, et al., A multiphase model for three-dimensional tumor growth, *New J. Phys.*, **15** (2013), 015005.

35. A. M. Stein, T. Demuth, D. Mobley, M. Berens, L. M. Sander, A mathematical model of glioblastoma tumor spheroid invasion in a three-dimensional in vitro experiment, *Biophys. J.*, **92** (2007), 356–365.

36. A. Tosin, L. Preziosi, Multiphase modeling of tumor growth with matrix remodeling and fibrosis, *Math. Comput. Model.*, **52** (2010), 969–976.

37. J. O. Waldeland, S. Evje, A multiphase model for exploring tumor cell migration driven by autologous chemotaxis, *Chem. Eng. Sci.*, **191** (2018), 268–287.

38. B. A. Webb, M. Chimenti, M. P. Jacobson, D. L. Barber, Dysregulated pH: a perfect storm for cancer progression, *Nat. Rev. Cancer*, **11** (2011), 671–677.

39. F. J. Wippold, M. Lämmle, F. Anatelli, J. Lennerz, A. Perry, Neuropathology for the neuroradiologist: Palisades and pseudopalisades, *AJNR Am. J. Neuroradiol.*, **27** (2006), 2037–2041.

40. S. M. Wise, J. S. Lowengrub, H. B. Frieboes, V. Cristini, Three-dimensional multispecies nonlinear tumor growth—I: Model and numerical method, *J. Theor. Biol.*, **253** (2008), 524–543.

Appendix

Non-dimensionalisation

The following rescalings of the dimensional quantities involved in the obtain equations are considered:

$$\tilde{h} := \frac{h}{h_{max}}, \qquad \tilde{t} := ta_3, \qquad \tilde{x} := x\sqrt{\frac{a_3}{D_H}} \qquad \tilde{c}_1 := \frac{c_1}{a_3}, \qquad \tilde{c}_2 := \frac{c_2}{a_3},$$

$$\tilde{c}_3 := \frac{c_3}{a_3}, \qquad \tilde{K}_{mn} := \frac{K_{mn}D_H}{\alpha_c}, \qquad \tilde{K}_{cm} := \frac{K_{cm}D_H}{\alpha_c}, \qquad \tilde{K}_{cn} := \frac{K_{cn}D_H}{\alpha_c},$$

$$\tilde{\chi} := \frac{\chi h_{max}}{\alpha_c}, \qquad \tilde{\alpha}_m := \frac{\alpha_m}{\alpha_c}, \qquad \tilde{a}_2 := \frac{a_2}{a_3 h_{max}}, \qquad \tilde{g}(\tilde{h}) := \frac{\tilde{\chi}\tilde{h}}{1+\tilde{h}},$$

$$\tilde{D}_{cc}(u_c, u_m, u_n) := (\tilde{K}_{cm}u_c + \tilde{K}_{mn}(1-u_c))(1-u_c) - (\tilde{K}_{cm} - \tilde{K}_{cn})u_c u_m,$$

$$\tilde{D}_{cm}(u_c, u_m, u_n) := -(\tilde{K}_{cm}u_c + \tilde{K}_{mn}(1-u_c))u_c + (\tilde{K}_{cm} - \tilde{K}_{cn})u_c(1-u_m),$$

$$\tilde{D}_{mc}(u_c, u_m, u_n) := -(\tilde{K}_{cm}u_m + \tilde{K}_{cn}(1-u_m))u_m + (\tilde{K}_{cm} - \tilde{K}_{mn})u_m(1-u_c),$$

$$\tilde{D}_{mm}(u_c, u_m, u_n) := (\tilde{K}_{cm}u_m + \tilde{K}_{cn}(1-u_m))(1-u_m) - (\tilde{K}_{cm} - \tilde{K}_{mn})u_c u_m,$$

$$\tilde{S}(u_c, u_m, u_n) := \tilde{K}_{cm}\tilde{K}_{cn}u_c + \tilde{K}_{cm}\tilde{K}_{mn}u_m + \tilde{K}_{cn}\tilde{K}_{mn}(1-u_c-u_m).$$

Dropping the tildes for simplicity, system (3.51), (3.11) writes in the nondimensional form as

$$\partial_t u_c = \nabla \cdot \left(\frac{1}{S(u_c, u_m, u_n)} \left[D_{cc}(2u_c + g(h)) + D_{cm}\alpha_m u_m^2 \theta \right] \nabla u_c \right)$$

$$+ \nabla \cdot \left(\frac{1}{S(u_c, u_m, u_n)} \left[D_{cc}u_c \nabla(g(h)) + 2D_{cm}\alpha_m u_m(1 + \theta u_c)\nabla u_m \right] \right) - c_1 u_c u_n(h-1), \qquad \text{(5.2a)}$$

$$\partial_t u_m = \nabla \cdot \left(\frac{1}{S(u_c, u_m, u_n)} \left[2D_{mm}\alpha_m u_m(1 + \theta u_c) \right] \nabla u_m, \right)$$

$$+ \nabla \cdot \left(\frac{1}{S(u_c, u_m, u_n)} \left[D_{mc}\nabla(u_c^2 + g(h)u_c) + D_{mm}\alpha_m \theta u_m^2 \nabla u_c \right] \right) - \frac{c_2 u_m(h-1)_+}{1 + u_m + h} - c_3 u_m, \qquad \text{(5.2b)}$$

$$\partial_t h = \Delta h + a_2 u_c - h, \qquad \text{(5.2c)}$$

$$u_n = 1 - u_c - u_m. \qquad \text{(5.2d)}$$

Parameters

The following table (see Table 1) summarises the parameters used in the simulations of Section 5.

Table 1. Parameters (dimensional quantities) involved in (3.51).

Parameter	Meaning	Value	Reference
h_{max}	acidity threshold for cancer cell death	$10^{-6.4}$ mol/L	[38]
a_2	proton production rate	10^{-9} mol /(L·s)	[27, 29]
a_3	proton removal rate	10^{-11} /s	[26]
D_h	acidity diffusion coefficient	$5 \cdot 10^{-14} - 10^{-11}$ m^2/s	[26, 27]
c_1	glioma growth/decay rate	$2.31 \cdot 10^{-6}$ /s	[13, 35]
c_2	normal cells decay rate	$3.47 \cdot 10^{-6}$ /s	this work
c_3	normal cells decay rate	$3.47 \cdot 10^{-8}$ /s	this work
K_{cm}	drag force coefficient between glioma and normal cells	$1.62 \cdot 10^{10}$ N m^{-4}s	this work
K_{mn}	drag force coefficient between normal and necrotic cells	$1.66 \cdot 10^{10}$ N m^{-4}s	this work
K_{cn}	drag force coefficient between glioma and normal cells	$1.7 \cdot 10^{10}$ N m^{-4}s	this work
χ	coefficient in the additional pressure on glioma due to acidity interaction	2.98 N m^{-2} L/mol	this work
θ	dimensionless coefficient in the additional pressure on normal cells due to glioma	1	this work
α_m	coefficient in the additional pressure on normal cells due to glioma	$1.49 \cdot 10^{-7}$ N m^{-2}	this work
α_c	coefficient in the additional pressure on glioma due to their crowding	$1.49 \cdot 10^{-7}$ N m^{-2}	this work